Fullerene-Free Polymer Solar Cells with over 11% Efficiency and Excellent Thermal Stability

Wenchao Zhao, Deping Qian, Shaoqing Zhang, Sunsun Li, Olle Inganäs, Feng Gao, and Jianhui Hou**

Solution-processed bulk heterojunction (BHJ) polymer solar cells (PSCs) have exhibited great potentials for making large area and flexible solar panels through low-cost solution coating techniques.[1–4] Typically, a BHJ active layer in a PSC is composed of a conjugated polymer as electron donor and an organic compound as electron acceptor.[5–9] Although fullerene derivatives, especially for [6,6]-phenyl-C_{71}-butyric acid methyl ester ($PC_{71}BM$), have been predominately used in highly efficient PSCs, nonfullerene (NF) acceptors have attracted much attention because of their easily tunable molecular energy levels, excellent optical absorption properties, and potential for low-cost production processes.[10–13] However, the power conversion efficiencies (PCEs) of the polymer:NF-acceptor-based PSCs (also known as fullerene-free PSCs)[14–29] are still lower than the state-of-art PCEs of the polymer:$PC_{71}BM$-based PSCs.[30–36]

A broad absorption spectrum is a prerequisite for achieving a high PCE in a photovoltaic cell. Since the photoactive materials used in PSCs, including conjugate polymers and small molecular compounds, usually possess comparatively narrow absorption spectra, the donor and acceptor used in a highly efficient PSC should have complementary absorption spectra so that the photoactive layer can efficiently absorb sunlight and generate more excitons, the electron–hole pairs bound by Coulomb interaction. In BHJ PSCs, the exciton dissociation process, during which the photogenerated excitons convert to free charges, plays a key role in the photon-to-electron conversion process.[6] During the exciton dissociation process in a BHJ blend film, electrons hop from the lowest unoccupied molecular orbital (LUMO) of the donor to the LUMO of the acceptor, and holes hop from the highest occupied molecular orbital (HOMO) of the acceptor to HOMO of donor; therefore, we need to minimize the energy loss during the exciton dissociation process so that the gaps of the $LUMO_{donor}$-$LUMO_{acceptor}$ (ΔLUMO) and the $HOMO_{donor}$-$HOMO_{acceptor}$ (ΔHOMO) are large enough to provide a driving force.[4,6,37] Compared to anisotropic acceptors, such as conjugated polymers or small molecular compounds, fullerene derivatives possess isotropic conjugated skeletons that allow for the easy formation of effective intermolecular π–π interactions with the anisotropic conjugated backbones of the polymer donors, causing the photovoltaic performance of the fullerene-free PSCs to be more susceptible to the donor:acceptor intermolecular arrangement of their BHJ active layers.[4,38] In fact, although many NF-acceptors with superior absorption spectra[26–28] and molecular energy level alignments[16,19–22] have been applied in PSCs, the PCEs of fullerene-free PSCs still lag behind those of fullerene-based PSCs.

Here, we demonstrate promising photovoltaic properties of fullerene-free PSCs using a new combination of a conjugated polymer (PBDB-T: poly[(2,6-(4,8-bis(5-(2-ethylhexyl)thiophen-2-yl)-benzo[1,2-b:4,5-b']dithiophene))-alt-(5,5-(1',3'-di-2-thienyl-5',7'-bis(2-ethylhexyl)benzo[1',2'-c:4',5'-c']dithiophene-4,8-dione))]) and small molecular compound (ITIC: 3,9-bis(2-methylene-(3-(1,1-dicyanomethylene)-indanone))-5,5,11,11-tetrakis(4-hexylphenyl)-dithieno[2,3-d:2',3'-d']-s-indaceno[1,2-b:5,6-b'] dithiophene) (see **Figure 1**a),[24,39] and we also prepared PBDB-T:$PC_{71}BM$-based PSCs as control samples. According to the absorption spectra shown in Figure 1b, the absorption spectrum of the PBDB-T film substantially overlaps that of the $PC_{71}BM$ spectrum in the visible range but is complementary with that of ITIC; therefore, the PBDB-T:ITIC blend film has a more favorable optical absorption than the PBDB-T:$PC_{71}BM$ blend film. We also measured the temperature-dependent absorption spectra of PBDB-T in chlorobenzene solution. As shown in Figure 1c, the PBDB-T solution shows a shoulder peak at temperatures below 90 °C, indicating that PBDB-T has a strong aggregation effect in solution. This is helpful for forming purer polymer aggregations and suppressing geminate recombination in a device.[31,39–42] The molecular energy level alignments in these two types of blends, which were determined by electrochemical cyclic voltammetry (see Figure S1, Supporting Information), are presented in Figure 1d. The ΔLUMO and ΔHOMO in the PBDB-T:ITIC blend are 0.86 and 0.18 eV, respectively, which are smaller (especially for the ΔHOMO) than those in the PBDB-T:$PC_{71}BM$ blend. Therefore, from the PBDB-T:$PC_{71}BM$ to the PBDB-T:ITIC, the energy loss during the exciton dissociation can be significantly reduced.

We fabricated PSCs with device structures of ITO(Indium tin oxide)/ZnO/BHJ-layer/MoO_3/Al, where the ZnO and MoO_3 were used to fabricate the *n*-type and *p*-type interlayers, respectively. The active layers of the PBDB-T:$PC_{71}BM$ control devices were fabricated as described in our previous work.[36,39,40] The optimal conditions for producing the PBDB-T:ITIC were obtained by scanning the PBDB-T:ITIC weight ratios; tuning the solvent compositions by mixing chlorobenzene with a trace amount

W. C. Zhao, S. Q. Zhang, S. S. Li, Prof. J. H. Hou
State Key Laboratory of Polymer Physics and Chemistry
Beijing National Laboratory for Molecular Sciences
Institute of Chemistry
Chinese Academy of Sciences
Beijing 100190, P. R. China
E-mail: hjhzlz@iccas.ac.cn
D. P. Qian, Prof. O. Inganäs, Prof. F. Gao
Biomolecular and Organic Electronics
IFM
Linköping University
Linköping 58183, Sweden
E-mail: fenga@ifm.liu.se

DOI: 10.1002/adma.201600281

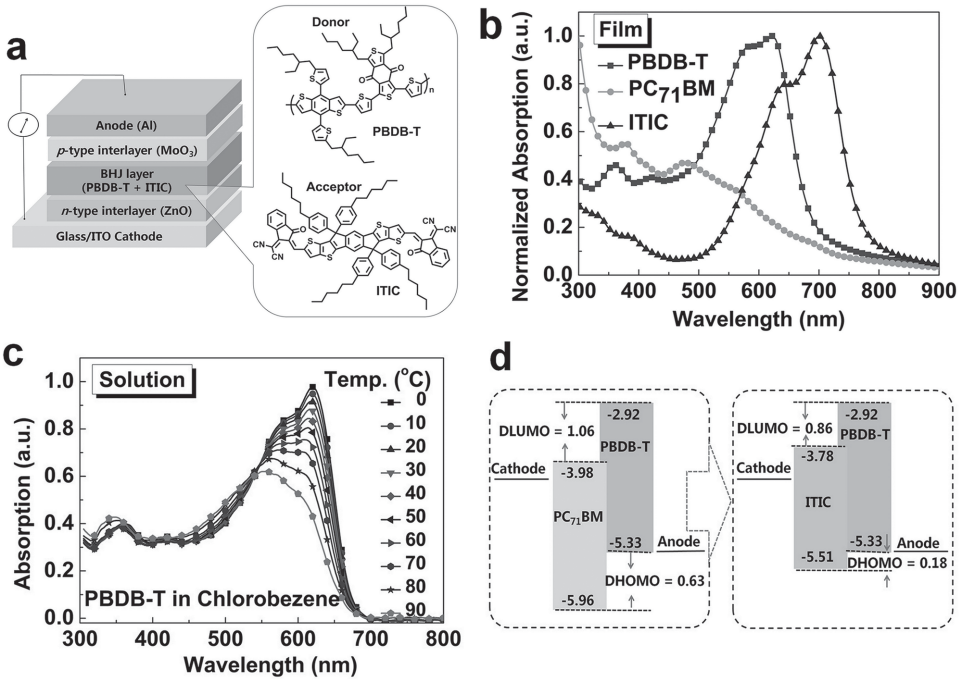

Figure 1. a) Device architecture and chemical structures of the donor and the acceptor used in this study. b) Normalized absorption spectra of the films. c) Temperature-dependent absorption spectra of the polymer PBDB-T in chlorobenzene solution. d) Molecular energy-level alignments in the devices based on PBDB-T:$PC_{71}BM$ and PBDB-T:ITIC.

of 1,8-diiodooctane (DIO) and then annealing the active layers under various temperatures (see Tables S1–S3 and Figure S2, Supporting Information). To determine the best-performing PSCs, the current-density/voltage (*J*–*V*) curves measured under simulated AM 1.5G, 100 mW cm^{-2} irradiance are shown in **Figure 2**a, and the corresponding parameters are listed in

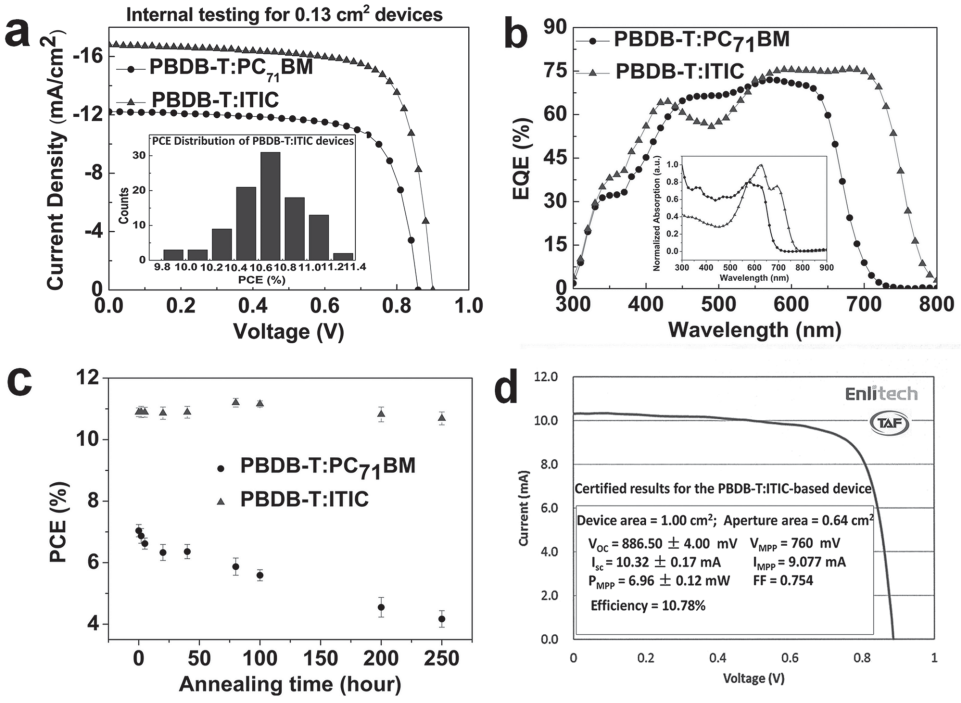

Figure 2. a) Current density versus voltage (*J*–*V*) curves obtained from our laboratory and histogram of PCE counts for 100 pieces of PBDB-T:ITIC-based cells (the inset). b) EQE curves and absorption spectra of PBDB-T:$PC_{71}BM$ and PBDB-T:ITIC blend film (the inset). c) PCEs of the devices after long-term annealing at 100 °C. d) Certified result of a 1 cm^2 PBDB-T:ITIC-based device.

Table 1. Photovoltaic parameters of the PBDB-T:ITIC-based solar cells.

	Cell area [cm^2]	V_{oc} [V]	J_{sc} [mA cm^{-2}]	FF	PCE [%]
Internal test for the best performing device[a)]	0.13	0.899	16.81	0.742	11.21
Statistical data of internal results[b)]	0.13	0.902 ± 0.006	16.73 ± 0.46	0.708 ± 0.01	10.68 ± 0.29
Certified results[c)]	1.00/0.64[d)]	0.887	16.12	0.754	10.78

[a)]The results for the best performing device prepared under the optimal conditions as provided in the Supporting Information; [b)]The statistical results of 100 cells obtained from five batches; [c)]The photovoltaic data collected from the test report provided by Enli Tech. Optoelectronic Calibration Lab; [d)]The cell area is 1.00 cm^2 and the aperture area is 0.64 cm^2.

Table 1. The PBDB-T:$PC_{71}BM$ control device showed a short-circuit current density (J_{sc}) of 12.80 mA cm^{-2}, an open-circuit voltage (V_{oc}) of 0.853 V, and a fill factor (FF) of 0.682, yielding a PCE of 7.45%, which coincides with the result obtained in our previous work.[36,39,40] The PBDB-T:ITIC device showed a J_{sc} of 16.80 mA cm^{-2}, an open-circuit voltage (V_{oc}) of 0.899 V, and an FF of 0.742, yielding a PCE of 11.21%. The external quantum efficiencies (h_{EQE}) as a function of the wavelength of the incident light of the two devices are shown in Figure 2b. Clearly, the PBDB-T:ITIC-based device exhibits a much broader response to sunlight, and the significantly improved J_{sc} can be attributed to the light absorption of ITIC. To further understand the J_{sc} and FF of the PBDB-T:ITIC device, we measured the electron and hole mobilities using the space-charge-limited current method with the device structures of ITO/ZnO/PBDB-T:ITIC/Al and ITO/PEDOT:PSS/PBDB-T:ITIC/Au, respectively. The electron and hole mobilities were 3.13×10^{-4} cm^2 V^{-1} s^{-1} and 2.10×10^{-4} cm^2 V^{-1} s^{-1}, respectively (see Figure S3, Supporting Information). The relatively low ratio of electron and hole mobility (μ_e/μ_h = 1.49) suggests a fairly balanced charge transport in PBDB-T:ITIC blend film, and thus a high J_{sc} and FF can be obtained in PBDB-T:ITIC-based devices.

In order to understand whether there is further room to improve the photovoltage, which is another key parameter which determines the device performance, we directly probed the interfacial energetics through the charge-transfer (CT) state, which is an intermolecular state formed between the donor and acceptor.[43,44] **Figure 3** shows the CT region of the EQE spectra and fits the CT band using Equation (1)

$$\mathrm{EQE}(E) \propto \frac{1}{E\sqrt{4\pi\lambda kT}} \exp\left(\frac{-(E_{CT}+\lambda-E)^2}{4\lambda kT}\right) \quad (1)$$

where k is the Boltzmann's constant, T is the absolute temperature, E_{CT} is the energy of CT states, and λ is related to the width of the CT absorbance band, with contributions from internal/environmental reorganization and/or energetic disorder. Advanced spectroscopic studies have suggested that it is desirable to have material combinations with low reorganization energies so that delocalized charge wave functions can be obtained.[45] Recent investigations of intermolecular arrangements emphasized the importance of a specific molecular configuration at the donor/acceptor interfaces to decrease the energetic disorder and increase the charge separation.[46] Our fitting shows an obvious difference in the values of λ (0.13 eV for the PBDB-T:ITIC blend and 0.30 eV for the PBDB-T:$PC_{71}BM$ blend). The low λ value of 0.13 eV of our PBDB-T:ITIC blend represents one of the narrowest CT absorbance bands measured in any BHJ system and suggests efficient charge generation regardless of its origin.[46]

The E_{CT} values from the fitting are 1.50 and 1.42 eV for the PBDB-T:ITIC and PBDB-T:$PC_{71}BM$ devices, respectively. The difference in the CT energy (1.50–1.42 = 0.08 eV) is consistent with the difference in the V_{oc} (0.06 V) of these two devices, and both are in good agreement with the empirical relation of $V_{OC} \approx E_{CT}/q - 0.6$.[47] The energy loss resulting from charge transfer is given by the difference between the energy of the excited pure components (E_{P*}) and the E_{CT}. The PBDB-T:ITIC blend shows a low E_{P*}–E_{CT} of 0.09 eV (1.59–1.50), which is among the lowest energy losses measured for any efficient charge-transfer process.[48–50] In contrast, for the PBDB-T:$PC_{71}BM$ blend, the E_{P*}–E_{CT} is as large as 0.35 eV (1.77–1.42 eV). The smaller E_{P*}–E_{CT} in the PBDB-T:ITIC blend also explains its higher V_{OC} value despite its smaller optical band gap relative to the PBDB-T:$PC_{71}BM$ blend. With such a low E_{P*}–E_{CT}, further improvements in the V_{OC} can only be achieved by removing the nonradiative recombination pathways,[44] which would decrease the V_{oc} by

$$\Delta V_{OC}^{\text{non-rad}} = -\frac{kT}{q}\ln(\mathrm{EQE}_{EL}) \quad (2)$$

where EQE_{EL} is radiative quantum efficiency of the solar cell when charge carriers are injected into the device in the dark. At room temperature, $\Delta V_{OC}^{\text{non-rad}}$ increases by 60 mV when the EQE_{EL} decreases by one order. The EQE_{EL} of the pure ITIC device is measured as 0.8×10^{-3}, and that of the polymer:nonfullerene blend is 1×10^{-6} (see Figure S4, Supporting Information). The significant difference in the EQE_{EL} values between the pure ITIC device and the PBDB-T:ITIC device constitutes the main contribution to the difference between the V_{oc} values of these

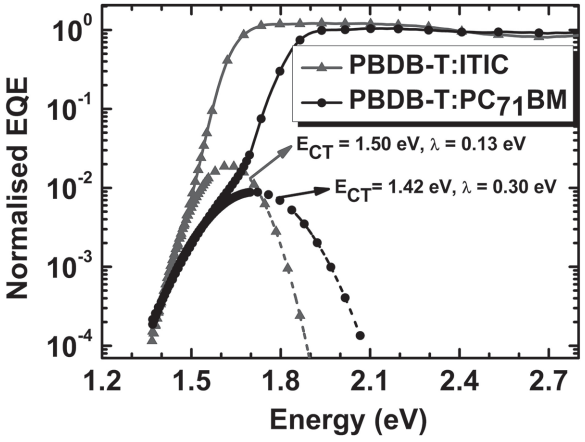

Figure 3. The EQE_{PV} spectra (in logarithmic scale) of PBDB-T:$PC_{71}BM$ and PBDB-T:ITIC based devices, respectively; the short dashed curves are the fitting curves with Equation (1) to obtain values for E_{CT} and λ.

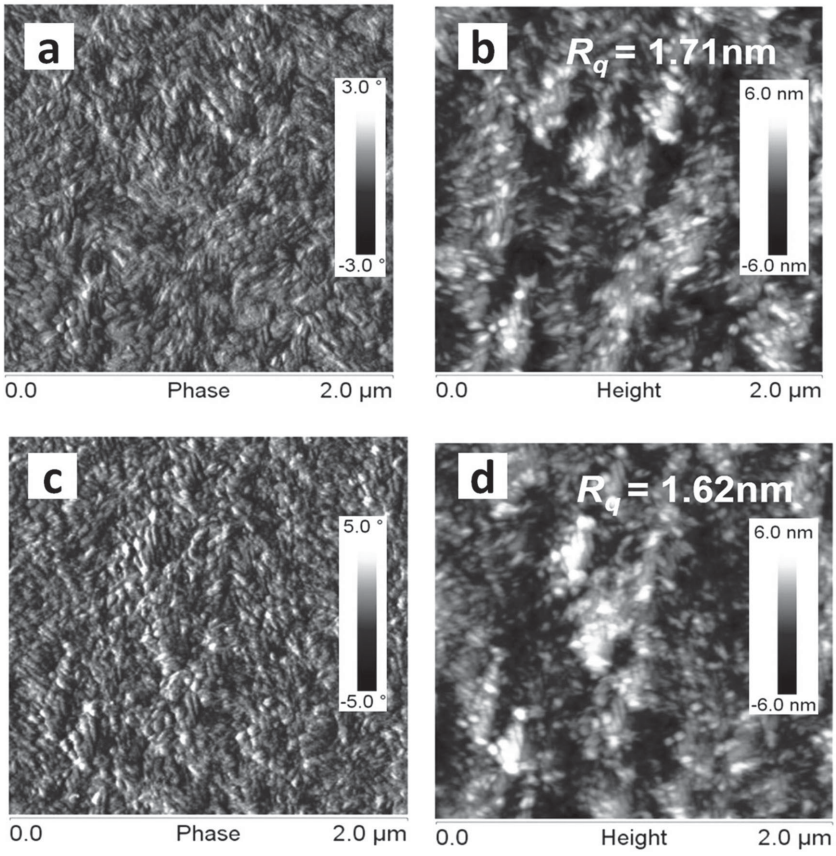

Figure 4. AFM phase images of (a) PBDB-T:$PC_{71}BM$ film and (c) PBDB-T:ITIC film and AFM height images of (b) PBDB-T:$PC_{71}BM$ film and (d) PBDB-T:ITIC film.

two devices (see Figure S5, Supporting Information), indicating a clear pathway to further improve the V_{oc} and the PCE.

We investigated the morphological properties of the films of the neat materials and the PBDB-T:$PC_{71}BM$ and PBDB-T:ITIC blends films using transmission electron microscopy (TEM) and tapping-mode atomic force microscopy (AFM). The neat PBDB-T, $PC_{71}BM$ and ITIC films show distinctly different surface and bulk morphologies (see Figure S6–S9, Supporting Information). The neat $PC_{71}BM$ film shows a very smooth surface (R_q = 0.24 nm), and the aggregate size observed at the surface and in the bulk is very small. In contrast, the ITIC film shows a rougher surface with R_q = 5.46 nm, and large irregular aggregates can be observed by TEM. Interestingly, as depicted in **Figure 4**a–d, the two blend films show very similar surfaces, i.e., the R_q of the two films are 1.71 and 1.62 nm, respectively, and granular aggregates of similar sizes can be observed in the two phase images. In the TEM measurements, the two films also exhibit similar phase-separation morphologies (see Figure S9, Supporting Information), which is beneficial for realizing efficient exciton dissociations in the device.[51–53] Based on the AFM and TEM observations, we infer that the phase-separation morphologies of the blended films are mainly determined by the polymer because PBDB-T may self-assemble to form nanoscale aggregates in solid neat films because of its strong aggregation effect in the solution state, as depicted vide supra. In fact, when we changed the solution temperature for spin coating, the photovoltaic performance of the devices was affected (see Table S4, Supporting Information), suggesting that the aggregation effect of the polymer in the solution state plays a critical role in achieving the aforementioned favorable phase-separation morphology.

As previously determined, in the polymer:$PC_{71}BM$ blends, $PC_{71}BM$ has a strong tendency to form large aggregates at high temperatures, and as a result, the polymer:$PC_{71}BM$-based solar cells usually have poor thermal stabilities.[54] We confirmed that the PBDB-T:ITIC devices have excellent thermal stabilities. For the PBDB-T:ITIC-based devices, when the active layers were annealed under 200 °C for 30 min, the corresponding device continued to exhibit a PCE of 10.0%; however, for the PBDB-T:$PC_{71}BM$-based devices, the PCE decreased to 3.4% under 200 °C for 30 min (see Figure S2, Supporting Information). We also checked the devices' long-term thermal stability. As shown in Figure 2c, after being annealed under 100 °C for 250 h, the PBDB-T:ITIC-based device still showed a PCE of 10.8%, while that of the PBDB-T:$PC_{71}BM$-based device dropped to 4.2%.

The photovoltaic performance of the PBDB-T:ITIC device is reproducible. For each batch of devices fabricated in our laboratory, we obtained 100 cells on 100 pieces of glass/ITO substrates. The PCE distribution of the devices made from the five batches under the optimal fabrication conditions is shown as the inset of Figure 2a. As listed in Table 1 and shown in Supporting Information Figure S10, the photovoltaic parameters of these devices show narrow standard deviations, i.e., V_{oc} = 0.902 ± 0.006 V, J_{sc} = 16.73 ± 0.46 mA cm^{-2}, and FF = 0.708 ± 0.01, and the resulting PCE = 10.68% ± 0.29%. Furthermore, fullerene-free PSCs with 1.00 cm^2 areas were fabricated and sent to Enli Tech. Optoelectronic Calibration Lab for certification. As demonstrated in Figure 2d and Figure S10 (Supporting Information), a rated efficiency of 10.78% was certified, and to the best of our knowledge, this is the highest value recorded not only for fullerene-free PSCs but also for any PSCs with an area of 1.00 cm^2.

In conclusion, we have demonstrated superior performance of PBDB-T:ITIC-based fullerene-free PSCs, providing the first example where the PCE of NF-based PSCs outperform that of fullerene-based PSCs. Compared to the PBDB-T:$PC_{71}BM$ blend, the PBDB-T:ITIC blend shows a much broader absorption band and a more appropriate molecular energy level alignment. The PBDB-T:ITIC-based PSCs show outstanding PCEs of up to 11.21% with excellent thermal stability, constituting substantial improvement relative to devices based on PBDB-T:$PC_{71}BM$ and a state-of-the-art PCE for PSCs. Furthermore, an efficiency of 10.78% was certified based on PBDB-T:ITIC device, and to the best of our knowledge, this is the highest value not only for fullerene-free PSCs but also for all types of PSCs with an area of 1.00 cm^2. Overall, the results of this work clearly confirm

that fullerene-free PSCs possess a high potential for advancing PSCs technology for practical applications and opening new avenues for the fundamental study of organic photovoltaics.

Experimental Section

Materials: PBDB-T was synthesized at ICCAS following the methods in our previous work.[39] The ZnO solution used to make the cathode buffer layers was synthesized according to the literature.[55] ITIC and $PC_{71}BM$ were purchased from Solarmer Materials Inc. Unless otherwise stated, all chemicals were commonly commercially available products and were used as received.

Device Fabrication: The device architecture was ITO/ZnO/PBDB-T:ITIC/MoO_3/Al. The ZnO layer was spin-coated on top of a precleaned, UV-ozone-treated ITO substrate. Subsequently, PBDB-T:ITIC (1:1 weight ratio) in a 20 mg mL^{-1} chlorobenzene:DIO (99.5:0.5 volume ratio) solution was spin-coated at 2500 rpm for 60 s to obtain a film thickness of ≈100 nm. Then, the device fabrication was completed by thermally evaporating 10-nm-thick MoO_3 and 100-nm-thick aluminum under vacuum at a pressure of 3×10^{-4} Pa. Lastly, the devices were encapsulated using UV epoxy and a glass cover in a nitrogen-protected glove box. To make the control devices, PBDB-T:$PC_{71}BM$ (1:1) in a 20 mg mL^{-1} dichlorobenzene:DIO (97:3) solution was spin-coated at 1000 rpm for 60 s to obtain a film thickness of ≈100 nm.

Device Measurement: The *J–V* curves were measured under AM1.5G illumination at 100 mW cm^{-2} using an AAA solar simulator (XES-70S1, SAN-EI Electric Co., Ltd) calibrated with a standard photovoltaic cell equipped with a KG5 filter (certificated by the National Institute of Metrology) and a Keithley 2400 source-measure unit. The EQE data were obtained using a solar cell spectral response measurement system (QE-R3011, Enli Technology Co. Ltd). The film thickness data were obtained via a surface profilometer (Dektak XT, Bruker). For the internal test of the 0.13 cm^2 devices, the device areas were defined by the mask used for the thermal evaporation, which was calibrated by the National Methodology Institute; for the certification testing, the device area was determined using a 0.64 cm^2 aperture on a 1.00 cm^2 device.

Supporting Information

Supporting Information is available from the Wiley Online Library or from the author.

Acknowledgements

The authors would like to acknowledge the financial support from the National Basic Research Program 973 (Grant No. 2014CB643501), the NSFC (Grant Nos. 91333204 and 21325419), the Chinese Academy of Sciences (Grant No. XDB12030200), the CAS-Croucher Funding Scheme for Joint Labs (CAS14601), and China Scholarship Council (CSC).

Received: January 17, 2016
Revised: February 21, 2016
Published online: April 9, 2016

[1] J. J. M. Halls, C. A. Walsh, N. C. Greenham, E. A. Marseglia, R. H. Friend, S. C. Moratti, A. B. Holmes, *Nature* **1995**, *376*, 498.
[2] G. Li, R. Zhu, Y. Yang, *Nat. Photonics* **2012**, *6*, 153.
[3] C. J. Brabec, N. S. Sariciftci, J. C. Hummelen, *Adv. Funct. Mater.* **2001**, *11*, 15.
[4] B. C. Thompson, J. M. J. Frechet, *Angew. Chem. Int. Ed.* **2008**, *47*, 58.
[5] N. S. Sariciftci, L. Smilowitz, A. J. Heeger, F. Wudl, *Science* **1992**, *258*, 1474.
[6] G. Yu, J. Gao, J. C. Hummelen, F. Wudl, A. J. Heeger, *Science* **1995**, *270*, 1789.
[7] M. Granstrom, K. Petritsch, A. C. Arias, A. Lux, M. R. Andersson, R. H. Friend, *Nature* **1998**, *395*, 257.
[8] Y. F. Li, *Acc. Chem. Res.* **2012**, *45*, 723.
[9] L. Ye, S. Q. Zhang, L. J. Huo, M. J. Zhang, J. H. Hou, *Acc. Chem. Res.* **2014**, *47*, 1595.
[10] A. Facchetti, *Mater. Today* **2013**, *16*, 123.
[11] X. W. Zhan, A. Facchetti, S. Barlow, T. J. Marks, M. A. Ratner, M. R. Wasielewski, S. R. Marder, *Adv. Mater.* **2011**, *23*, 268.
[12] P. Sonar, J. P. Fong Lim, K. L. Chan, *Energy Environ. Sci.* **2011**, *4*, 1558.
[13] Y. Lin, X. Zhan, *Mater. Horiz.* **2014**, *1*, 470.
[14] Y. Zhou, T. Kurosawa, W. Ma, Y. K. Guo, L. Fang, K. Vandewal, Y. Diao, C. G. Wang, Q. F. Yan, J. Reinspach, J. G. Mei, A. L. Appleton, G. I. Koleilat, Y. L. Gao, S. C. B. Mannsfeld, A. Salleo, H. Ade, D. H. Zhao, Z. N. Bao, *Adv. Mater.* **2014**, *26*, 3767.
[15] L. Ye, W. Jiang, W. Zhao, S. Zhang, D. Qian, Z. Wang, J. Hou, *Small* **2014**, *10*, 4658.
[16] Y. Zang, C.-Z. Li, C.-C. Chueh, S. T. Williams, W. Jiang, Z.-H. Wang, J.-S. Yu, A. K. Y. Jen, *Adv. Mater.* **2014**, *26*, 5708.
[17] E. Zhou, J. Cong, K. Hashimoto, K. Tajima, *Adv. Mater.* **2013**, *25*, 6991.
[18] Y. Zhong, M. T. Trinh, R. Chen, W. Wang, P. P. Khlyabich, B. Kumar, Q. Xu, C.-Y. Nam, M. Y. Sfeir, C. Black, M. L. Steigerwald, Y.-L. Loo, S. Xiao, F. Ng, X. Y. Zhu, C. Nuckolls, *J. Am. Chem. Soc.* **2014**, *136*, 15215.
[19] J. Zhao, Y. Li, H. Lin, Y. Liu, K. Jiang, C. Mu, T. Ma, J. Y. Lin Lai, H. Hu, D. Yu, H. Yan, *Energy Environ. Sci.* **2015**, *8*, 520.
[20] L. Ye, K. Sun, W. Jiang, S. Zhang, W. Zhao, H. Yao, Z. Wang, J. Hou, *ACS Appl. Mater. Interfaces* **2015**, *7*, 9274.
[21] S. Li, H. Zhang, W. Zhao, L. Ye, H. Yao, B. Yang, S. Zhang, J. Hou, *Adv. Energy Mater.* **2015**, DOI: 10.1002/aenm.201501991.
[22] T. Kim, J.-H. Kim, T. E. Kang, C. Lee, H. Kang, M. Shin, C. Wang, B. Ma, U. Jeong, T.-S. Kim, B. J. Kim, *Nat. Commun.* **2015**, *6*, 8547.
[23] Y.-J. Hwang, H. Li, B. A. E. Courtright, S. Subramaniyan, S. A. Jenekhe, *Adv. Mater.* **2016**, *28*, 124.
[24] Y. Z. Lin, J. Y. Wang, Z. G. Zhang, H. T. Bai, Y. F. Li, D. B. Zhu, X. W. Zhan, *Adv. Mater.* **2015**, *27*, 1170.
[25] J. W. Jung, J. W. Jo, C. C. Chueh, F. Liu, W. H. Jo, T. P. Russell, A. K. Y. Jen, *Adv. Mater.* **2015**, *27*, 3310.
[26] H. Lin, S. Chen, Z. Li, J. Y. L. Lai, G. Yang, T. McAfee, K. Jiang, Y. Li, Y. Liu, H. Hu, J. Zhao, W. Ma, H. Ade, H. Yan, *Adv. Mater.* **2015**, *27*, 7299.
[27] L. Gao, Z.-G. Zhang, L. Xue, J. Min, J. Zhang, Z. Wei, Y. Li, *Adv. Mater.* **2015**, *28*, 1884.
[28] D. Meng, D. Sun, C. Zhong, T. Liu, B. Fan, L. Huo, Y. Li, W. Jiang, H. Choi, T. Kim, J. Y. Kim, Y. Sun, Z. Wang, A. J. Heeger, *J. Am. Chem. Soc.* **2016**, *138*, 375.
[29] Y. Zhong, M. T. Trinh, R. Chen, G. E. Purdum, P. P. Khlyabich, M. Sezen, S. Oh, H. Zhu, B. Fowler, B. Zhang, W. Wang, C. Y. Nam, M. Y. Sfeir, C. T. Black, M. L. Steigerwald, Y. L. Loo, F. Ng, X. Y. Zhu, C. Nuckolls, *Nat. Commun.* **2015**, *6*, 8242.
[30] L. Ye, S. Zhang, W. Zhao, H. Yao, J. Hou, *Chem. Mater.* **2014**, *26*, 3603.
[31] Y. Liu, J. Zhao, Z. Li, C. Mu, W. Ma, H. Hu, K. Jiang, H. Lin, H. Ade, H. Yan, *Nat. Commun.* **2014**, *5*, 5293.
[32] S. Q. Zhang, L. Ye, W. C. Zhao, B. Yang, Q. Wang, J. H. Hou, *Sci. China Chem.* **2015**, *58*, 248.
[33] J. D. Chen, C. H. Cui, Y. Q. Li, L. Zhou, Q. D. Ou, C. Li, Y. F. Li, J. X. Tang, *Adv. Mater.* **2015**, *27*, 1035.

[34] Z. C. He, B. Xiao, F. Liu, H. B. Wu, Y. L. Yang, S. Xiao, C. Wang, T. P. Russell, Y. Cao, *Nat. Photonics* **2015**, *9*, 174.
[35] W. C. Zhao, L. Ye, S. Q. Zhang, H. F. Yao, M. L. Sun, J. H. Hou, *J. Phys. Chem. C* **2015**, *119*, 27322.
[36] W. C. Zhao, L. Ye, S. Q. Zhang, M. L. Sun, J. H. Hou, *J. Mater. Chem. A* **2015**, *3*, 12723.
[37] M. C. Scharber, D. Wuhlbacher, M. Koppe, P. Denk, C. Waldauf, A. J. Heeger, C. L. Brabec, *Adv. Mater.* **2006**, *18*, 789.
[38] L. Ye, X. C. Jiao, M. Zhou, S. Q. Zhang, H. F. Yao, W. C. Zhao, A. D. Xia, H. Ade, J. H. Hou, *Adv. Mater.* **2015**, *27*, 6046.
[39] D. P. Qian, L. Ye, M. J. Zhang, Y. R. Liang, L. J. Li, Y. Huang, X. Guo, S. Q. Zhang, Z. A. Tan, J. H. Hou, *Macromolecules* **2012**, *45*, 9611.
[40] W. C. Zhao, L. Ye, S. Q. Zhang, B. H. Fan, M. L. Sun, J. H. Hou, *Sci. Rep.* **2014**, *4*, 6570.
[41] K. R. Graham, C. Cabanetos, J. P. Jahnke, M. N. Idso, A. El Labban, G. O. N. Ndjawa, T. Heumueller, K. Vandewal, A. Salleo, B. F. Chmelka, A. Amassian, P. M. Beaujuge, M. D. McGehee, *J. Am. Chem. Soc.* **2014**, *136*, 9608.
[42] W. Ma, G. F. Yang, K. Jiang, J. H. Carpenter, Y. Wu, X. Y. Meng, T. McAfee, J. B. Zhao, C. H. Zhu, C. Wang, H. Ade, H. Yan, *Adv. Energy Mater.* **2015**, *5*, 1501400.
[43] L. Goris, A. Poruba, L. Hod'akova, M. Vanecek, K. Haenen, M. Nesladek, P. Wagner, D. Vanderzande, L. De Schepper, J. V. Manca, *Appl. Phys. Lett.* **2006**, *88*, 052113.
[44] K. Vandewal, K. Tvingstedt, A. Gadisa, O. Inganas, J. V. Manca, *Phys. Rev. B* **2010**, *81*, 125204.
[45] A. A. Bakulin, A. Rao, V. G. Pavelyev, P. H. M. van Loosdrecht, M. S. Pshenichnikov, D. Niedzialek, J. Cornil, D. Beljonne, R. H. Friend, *Science* **2012**, *335*, 1340.
[46] K. R. Graham, C. Cabanetos, J. P. Jahnke, M. N. Idso, A. El Labban, G. O. N. Ndjawa, T. Heumueller, K. Vandewal, A. Salleo, B. F. Chmelka, A. Amassian, P. M. Beaujuge, M. D. McGehee, *J. Am. Chem. Soc.* **2014**, *136*, 9608.
[47] K. Vandewal, K. Tvingstedt, A. Gadisa, O. Inganas, J. V. Manca, *Nat. Mater.* **2009**, *8*, 904.
[48] K. Kawashima, Y. Tamai, H. Ohkita, I. Osaka, K. Takimiya, *Nat. Commun.* **2015**, *6*, 10085.
[49] W. W. Li, K. H. Hendriks, A. Furlan, M. M. Wienk, R. A. J. Janssen, *J. Am. Chem. Soc.* **2015**, *137*, 2231.
[50] N. A. Ran, J. A. Love, C. J. Takacs, A. Sadhanala, J. K. Beavers, S. D. Collins, Y. Huang, M. Wang, R. H. Friend, G. C. Bazan, T. Q. Nguyen, *Adv. Mater.* **2015**, *28*, 1482.
[51] J. K. Lee, W. L. Ma, C. J. Brabec, J. Yuen, J. S. Moon, J. Y. Kim, K. Lee, G. C. Bazan, A. J. Heeger, *J. Am. Chem. Soc.* **2008**, *130*, 3619.
[52] C. V. Hoven, X. D. Dang, R. C. Coffin, J. Peet, T. Q. Nguyen, G. C. Bazan, *Adv. Mater.* **2010**, *22*, E63.
[53] Y. Huang, E. J. Kramer, A. J. Heeger, G. C. Bazan, *Chem. Rev.* **2014**, *114*, 7006.
[54] M. Jorgensen, K. Norrman, F. C. Krebs, *Sol. Energy Mater. Sol. C* **2008**, *92*, 686.
[55] Y. M. Sun, J. H. Seo, C. J. Takacs, J. Seifter, A. J. Heeger, *Adv. Mater.* **2011**, *23*, 1679.